

Time-Resolved Measurements of Intramolecular Energy Transfer in Single Donor/Acceptor Dyads

G. Hinze,^{*,†} M. Haase,[†] F. Nolde,[‡] K. Müllen,[‡] and Th. Basché[†]

Institute for Physical Chemistry, Johannes Gutenberg-University, Jakob-Welderweg 11, D-55099 Mainz, Germany, and Max-Planck-Institute for Polymer Research, D-55128, Mainz, Germany

Received: April 22, 2005; In Final Form: June 9, 2005

We have investigated electronic excitation energy transfer in a specifically designed bichromophoric donor/acceptor dyad in which the donor (perylene diimide) and acceptor (terrylene diimide) are linked by a rigid heptaphenyl-spacer. Because of the choice of the bridge, which defines the distance and orientation of the two chromophores, donor as well as acceptor emission is observed. The significantly smaller photostability of the donor allows for time-resolved measurements of the acceptor emission at the single-molecule level with and without energy transfer from the donor. By analyzing the differences of the rise/decay profiles for both pathways, we could determine time constants of energy transfer with high accuracy for single dyads. The results show that the experimental approach presented here works even for situations in which the energy transfer times are smaller than the temporal resolution of the detection system.

Introduction

Electronic excitation energy transfer (EET) plays a key role in a wide variety of molecular assemblies.¹ The functioning of light-harvesting complexes and conjugated polymers crucially depends on the efficiency of this process.^{2–5} Furthermore, because EET between a donor (D) and an acceptor (A) chromophore sensitively depends on their distance and relative orientation,⁶ it constitutes a nanoscopic ruler⁷ on length scales between 10 and 100 Å. As a more special application, energy transfer between spatially confined D/A-couples has been used for probing the microstructure⁸ of the environment. Recently, EET at the single-molecule level has been applied to measure distances and distance fluctuations on the nanometer scale. Such EET between a single donor and a single acceptor pair turns out to be a powerful tool for visualizing the dynamics of (biological) macromolecules^{9–11} in real time and without the problems encountered by ensemble averaging. Other single-molecule investigations have focused on coupling mechanisms and more principal photophysical aspects of the energy transfer process.^{12–17} In this case, the lack of ensemble averaging turns out to be most helpful for comparing experimental results to theoretical predictions of electronic coupling.

To study fundamental aspects of EET, simple model systems¹⁸ are of particular importance. Recently, we have synthesized simple D/A dyads consisting of perylene diimide (PDI; D) and terylene diimide (TDI; A) separated by rigid oligophenyl spacers. The particular suitability of such compounds for studying EET at the single-molecule level results mainly from two facts. First, perylene diimide dyes exhibit extraordinary advantageous properties for single-molecule studies¹⁹ because they possess very high photostabilities and fluorescence quantum yields up to unity.^{20,21} Second, the combination with appropriate synthetic concepts enables us to build donor–acceptor (D/A) dyads, in which the distance and orientation between the PDI

donor and the TDI acceptor can be adjusted. As a first model system, we had studied a dyad in which PDI and TDI are separated by a *p*-terphenyl spacer.²² Because of the large spectral overlap, favorable dipole orientation, and short interchromophore distance, energy is transferred quantitatively from D to A in this dyad. Although the 3D orientation of the donor and acceptor absorption transition dipoles could be determined,²² the rate constant of the energy transfer process was too fast to be measured reliably by room-temperature single-molecule experiments. By varying the length and geometry of the spacer, the energy transfer efficiency can be tuned. In Scheme 1, the chemical structure of another dyad (**1**), in which PDI and TDI are now linked by a longer heptaphenyl-spacer including a kink, is presented. Please note that with respect to a dyad with a linear *p*-terphenyl spacer only the distance and orientation of the D/A couple has changed; the average spectral overlap is the same for both dyads.

In a recent investigation of single polyphenylene dendrimers, containing a central TDI acceptor core and being decorated by four perylenemonoimide donors, the acceptor rise time, which corresponds to an average over the energy transfer times of the four donors, was accessed by time-resolved fluorescence spectroscopy.²³ For the same multichromophoric dendrimer, we have shown that the energy transfer times of individual donors are readily accessible by fluorescence excitation spectroscopy at low temperatures.²⁴ In the following, we will demonstrate that bichromophoric dyad **1** allows for another type of measurement to determine the energy transfer time by time-resolved spectroscopy. It is based on differences of the fluorescence rise/decay time profiles recorded successively for a dyad prior to and after bleaching of the donor (PDI).

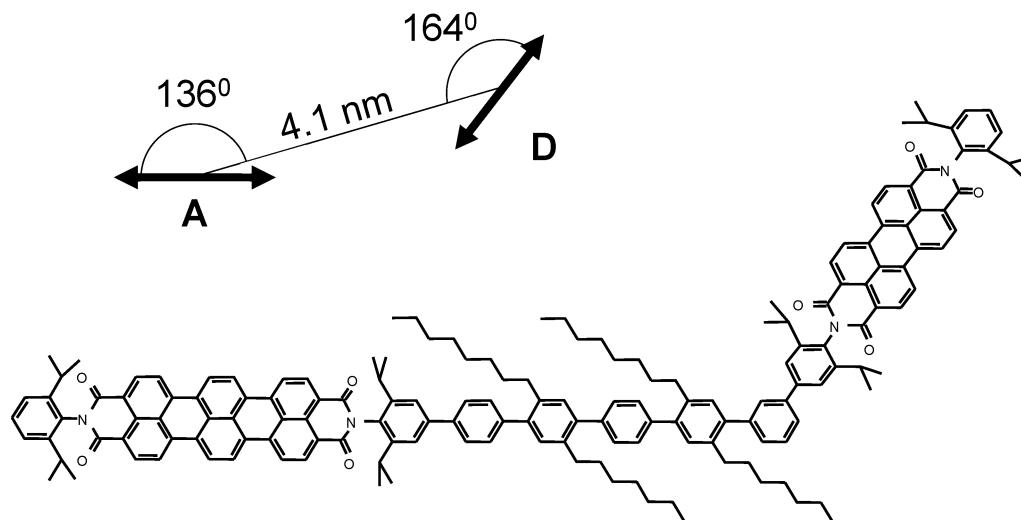
Experimental Section

The synthesis of dyad **1** will be published elsewhere.²⁵ For the single-molecule experiments, thin-films of PMMA (~70 nm) doped with the dyad were prepared by spin coating from solution on a cleaned glass substrate. From single-molecule confocal fluorescence microscopy, an average density of D/A couples

* Corresponding author. E-mail: hinze@mail.uni-mainz.de.

[†] Institute for Physical Chemistry, Johannes Gutenberg-University.

[‡] Max-Planck-Institute for Polymer Research.

SCHEME 1: Molecular Structure of **1**

of $\sim 0.3 \mu\text{m}^{-2}$ was obtained. Transient fluorescence intensities were taken with a home-built scanning confocal optical microscope. For excitation, we used either a cw-Ar ionlaser (488 nm) or a pulsed, frequency doubled Nd:YLF laser at 523 nm with a repetition rate of 40 MHz and pulse widths of about 4 ps. Compared to the 488 nm excitation that was used for the spectra shown in Figure 1, the longer wavelength increases the absorption probability of TDI, which turned out to be essential for the present investigations. An average excitation power of 3.5 kWcm^{-2} of circular polarized light turned out to be a good compromise between a sufficient signal-to-noise ratio in emission and a tolerable photobleaching efficiency. Emitted photons were collected by an oil immersion objective (100 \times , NA 1.4, Zeiss), which also was used for excitation. The detection path was divided by a 50/50 beam splitter with subsequent filtering. For the TDI emission, a long-pass filter was used (HQ700, Chroma), whereas for the PDI emission a band-pass filter (HQ570/60, Chroma) was incorporated. Time correlated single photon counting (TCSPC) was performed by two avalanche photodiodes (SPCM-AQ 14, Perkin-Elmer) followed by a PC module (Becker&Hickl) incorporating a time-to-amplitude converter (TAC) and an analog-to-digital converter (ADC) on board. All of the measurements were made at room temperature under air.

Results and Discussion

From quantum mechanical calculations (vacuum), the length of the connection vector between the centers of gravity of the

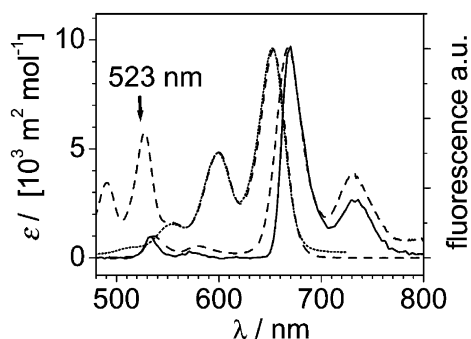


Figure 1. Absorption and emission spectra of a toluene solution of **1** (dashed lines). The dotted line represents the absorption spectrum of a toluene solution of TDI. A single-molecule emission spectrum of **1** in PMMA is drawn as a solid line ($\lambda_{\text{exc}} = 488 \text{ nm}$).

two chromophores was found to be $d_{da} = 4.1 \text{ nm}^{26}$ and the angle at the kink to be $\Theta_{da} = 120^\circ$. Both the distance between the chromophores and their relative orientation were chosen such that the expected transfer efficiency should be less than unity. Accordingly, the ensemble spectra of **1** in toluene show donor as well as acceptor emission (Figure 1). By scanning thin PMMA films doped with **1** in the confocal fluorescence microscope, single dyads were localized. The emission spectra of single, isolated dyads (Figure 1) confirmed that the PDI emission stems from intact dyads and not from unbound PDI.

It is important to note that the analysis of donor and acceptor emission intensities obtained from single-molecule experiments with **1** would not allow for a straightforward calculation of the EET efficiency. By embedding **1** in PMMA, the emission transition dipoles of PDI and TDI are fixed and, because of the kink in this dyad, oriented differently in space. Orientation-dependent detection sensitivity²⁷ and interfacial effects due to our thin sample geometry prevent a simple data analysis.²⁸

For the following experiments, excitation was performed at 523 nm employing the pulsed Nd:YLF laser. Only the brightest molecules with at least 50% of the maximum emission rate detected overall have been selected for further data evaluation. A simple analysis indicates that such a selection favors D/A pairs with a proper orientation of the donors' absorption transition dipole with respect to the excitation beam polarization. As already mentioned, for an intact dyad both PDI and TDI emission are observed (see Figure 1). Typically, after some time PDI bleaches preferentially, although the excitation is transferred quickly to the TDI acceptor. This observation is in accordance with studies on isolated PDI and TDI in PMMA, which showed that under our experimental conditions PDI bleached 100–1000 times faster than TDI.²⁹ After photobleaching of PDI, the residual absorption of TDI at the laser wavelength of 523 nm (see Figure 1) allows for direct excitation of this chromophore. Although the emission intensity dropped by a factor of ~ 10 , because of longer recording times the photon numbers were still sufficient for applying the time-correlated single photon counting (TCSPC) technique. As an example in Figure 2, a typical time trace is shown in which PDI bleached after $\sim 45 \text{ s}$. TDI emission via direct excitation was recorded for another 1200 s.

The scenario just described has one particularly important consequence. We are able to measure the rise/decay time profiles of the TDI emission for two different excitation pathways within

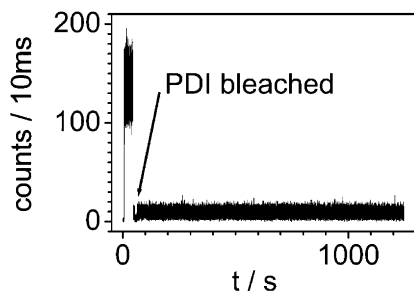


Figure 2. Time trace of single dyad **1** excited at 523 nm. After 45 s, PDI bleached first. Subsequently, because of the weak absorption of TDI at 523 nm, the emission intensity dropped by a factor of ~ 10 . After ~ 1250 s, the experiment was stopped. The corresponding rise/decay profile is shown in Figure 3.

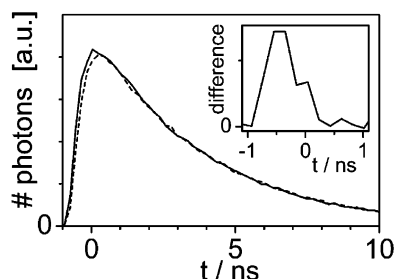


Figure 3. Fluorescence rise/decay time profiles for single dyad **1** excited at 523 nm before (dashed line) and after (solid line) photobleaching of the donor PDI. The profiles consist of 2.6×10^5 (before bleaching of PDI) and 3.9×10^5 counts (after bleaching of PDI), respectively. The inset shows the difference between both curves after normalizing to the long time tail. The corresponding time trace is shown in Figure 2.

a few seconds. By comparing rise/decay time profiles with and without transfer from PDI, the EET contribution can be isolated in single dyads. It is noted that this kind of experiment can only be performed at the single-molecule level.

In Figure 3, the fluorescence rise/decay time profiles are shown for a single dyad before and after photobleaching of the donor. Normalization to the long time decay allows for calculating the difference that solely stems from EET. Our main experimental limitation is given by the instrumental response function (IRF), which is basically determined by the relatively slow single photon avalanche photodiodes. From reflection measurements of the pump pulse, we obtain an IRF with a full width at half-maximum (fwhm) of ~ 700 ps. Although the EET turned out to be significantly faster (see below), the contribution from EET is clearly visible.

In recent work on the already mentioned single polyphenylene dendrimers, containing a central TDI acceptor core and being decorated by four perylenemonoimide donors, energy transfer had also been investigated by TCSPC.²³ Transfer times could be obtained by deconvolution of the fluorescence rise/decay time histograms using a microchannel plate multiplier with a response time of 23 ps. Our time resolution, which is limited by the rather slow APD, would not allow for this kind of data analysis. However, the use of a bichromophoric D/A dyad together with its particular photophysical properties, namely, the significantly higher photostability of the acceptor TDI compared to PDI, enables us to use a different approach to extract energy transfer times from single-molecule time-resolved data. Similar to the data analysis for the dendrimers,²³ we assume a biexponential model function with positively and negatively contributing time constants for the intact dyad. Accordingly, the fluorescence signals of the intact (1) and the PDI bleached (2) dyad are

described by

$$I_1(t) = \left[A_1 \exp\left(-\frac{t}{\tau_1}\right) - B_1 \exp\left(-\frac{t}{\tau_{\text{EET}}}\right) \right] \otimes \text{IRF}(t) \quad (1)$$

$$I_2(t) = A_2 \exp\left(-\frac{t}{\tau_2}\right) \otimes \text{IRF}(t) \quad (2)$$

Interestingly, in the D/A dendrimer comparable preexponential factors, $A_1 \approx B_1$, were found,²³ which point to an exclusive excitation of the donor followed by population of the TDI excited state via energy transfer. In our dyad **1**, however, to some extent direct excitation of the acceptor also takes place. From analyzing two step time traces as shown in Figure 2, we estimated the probability for the direct excitation path to be $\sim 10\%$, which corresponds to $0.9A_1 \approx B_1$. This estimate is in accordance with the absorption strength of PDI and TDI at 523 nm, taking into account that no polarization dependence has to be considered. The latter argument is based on the use of circular polarized excitation and the fact that preferential dyads are selected that are oriented parallel to the interface, that is, to the polarization plane of the laser light (see below). After normalization $A_1 = A_2 = 1$ and subsequently $B_1 = 1$, and assuming unchanged fluorescence lifetimes of the acceptor $\tau_1 = \tau_2$ the difference $\Delta(t)$ is given by

$$\Delta(t) = I_2(t) - I_1(t) = \exp\left(-\frac{t}{\tau_{\text{EET}}}\right) \otimes \text{IRF}(t). \quad (3)$$

The convolution in eq 3 can be solved to yield

$$\Delta(t) = \tau_{\text{EET}} \sum_{n=0}^{\infty} (-\tau_{\text{EET}})^n \left(\frac{d}{dt}\right)^n \text{IRF}(t) \quad (4)$$

In the first step of data evaluation, the fluorescence decay histogram of the TDI emission *after* bleaching of PDI was analyzed, that is, when TDI was excited directly by the 523-nm pulses. At times longer than ~ 1 ns, a strictly single-exponential decay was found for all of the molecules investigated. Within a minimization procedure using MATLAB package (Mathworks), we adjusted the instrumental response IRF to fit eq 2 to the experimental data. In the next step, the fluorescence rise/decay histogram of the intact dyad, that is, prior bleaching of PDI, was analyzed using the same IRF and eq 1. We want to emphasize that both steps were always performed with data obtained from the same molecule within a few seconds up to minutes without changing the experimental setup at all. Because the emission originates from TDI in both cases, our assumption that the IRF is the same for both cases seems to be justified.

Interestingly, even for short energy transfer times, $\tau_{\text{EET}} < 700$ ps, $\Delta(t)$ in a first approximation is proportional to the time constant, τ_{EET} . Consequently, energy transfer times significantly faster than the relatively poor temporal resolution of our setup could be extracted. In practice, the shortest accessible transfer times are determined eventually by the signal-to-noise ratio, which depends on the number of photons counted. Approximately half of the dyads investigated allowed for an extraction of EET times as described. As a lower limit, we required at least 2×10^4 counts for each fluorescence rise/decay histogram. For the remaining dyads, photobleaching of TDI either before or after PDI photobleaching prevented further data analysis. As mentioned above, in the majority of cases the emission intensity dropped by a factor of ~ 10 after bleaching of PDI. Consequently, to acquire similar photon numbers, the time traces

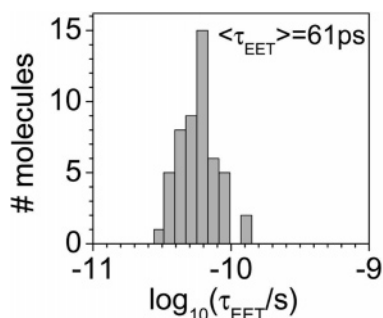


Figure 4. Distribution of energy transfer times obtained for 51 single dyads **1** in a thin PMMA film.

recorded after PDI bleaching were taken approximately 10 times longer than prior bleaching (see Figure 2).

In Figure 4, the EET times obtained from analyzing 51 single dyads are plotted. From this histogram, we obtain a mean transfer time of $\langle \tau_{\text{EET}} \rangle = (61 \pm 18)$ ps. This broad distribution of energy transfer times in Figure 4 is quite remarkable in light of the rigid geometry of **1**. It is therefore unreasonable to assume that the distribution reflects large variations in distance and relative orientation of donor and acceptor in the dyads; rather, it is thought to be caused by inhomogeneous broadening of the electronic transitions of both PDI and TDI. The (static) spectral shifts due to inhomogeneous broadening lead to variations of the spectral overlap for every single dyad. This very fact has been emphasized by Scholes¹ recently. However, to experimentally prove this assumption, the absorption spectra for each single dyad have to be known.

Assuming a classical Förster type process,⁶ energy transfer times can be calculated according to the following equation

$$\tau_{\text{EET}}^{-1} = k^{\text{Förster}} = \frac{\phi_{\text{D}}(R_0)^6}{\tau_{\text{D}}(R)^6} = \frac{\phi_{\text{D}}}{\tau_{\text{D}}} \frac{1}{R^6} \left(\frac{5.29 \times 10^{-4} \kappa^2 J(\lambda)}{Nn^4} \right) \quad (5)$$

$\kappa^2 = 2.5$ is the orientation factor associated with the dipole–dipole interaction between donor and acceptor,^{1,27} $R = 4.1 \times 10^{-9}$ m is their center-to-center separation, N is Avogadro's number, and $n = 1.49$ is the refractive index of PMMA. $\phi_{\text{D}} = 1$ is the donor fluorescence quantum yield,²⁰ and $\tau_{\text{D}} = 4.1$ ns is its measured fluorescence lifetime,²⁹ which is close to recently published data.³⁰ The spectral overlap $J(\lambda) = 2.47 \times 10^{-22}$ m⁶mol⁻¹ was obtained from a convolution of the bulk absorption spectrum of TDI in units of m²mol⁻¹ with the area-normalized emission spectrum of PDI (both solved in toluene). The transition dipoles for absorption and emission are assumed to be collinear with the long axes of the chromophores. We obtain a Förster radius of $R_0 = 6.9$ nm and a transfer efficiency of 96% corresponding to a transfer time of $\tau_{\text{EET}}^{\text{Förster}} = 164$ ps.

Because single-molecule emission (donor) and absorption spectra (acceptor) are not easily available for each single dyad, the calculation of the Förster radius or the spectral overlap, respectively, was based on ensemble averaged data from the constituent chromophores in toluene solution. Although the emission spectrum of a single dyad in PMMA does not differ too much from the ensemble emission spectrum in toluene solution (Figure 1), because of the lack of the actual spectral data, a discussion of the discrepancy between the transfer time calculated from Förster theory based on solution data and the mean energy transfer time obtained from single-molecule experiments in PMMA can at present only be done on a qualitative level.

A Förster radius of $R_0^* = 8.1$ nm would be needed to match the measured and calculated transfer times, which differ by a

factor of 2–3. With regard to the orientation factor, κ^2 , which is determined solely by the relative orientation of the transition dipoles of donor and acceptor, because $\tau_{\text{EET}}^{\text{Förster}} \propto \kappa^{-2}$, a theoretically impossible value of $\kappa^2 > 4$ would be required. Theoretical³¹ and experimental investigations²⁸ have shown the strong influence of a close interface on the fluorescence lifetime of single fluorophores.^{32,33} However, the measured transfer times would require a donor fluorescence lifetime of about $\tau_{\text{D}}^* = 1.5$ ns, which is beyond the conceivable range.

Within a simulation taking into account our film thickness of 70 nm, we calculated the influence of the air/PMMA interface on the EET times for 10^7 molecules randomly distributed and oriented in the film. Interestingly, by picking out only the brightest dyads, a selection concerning the molecular orientation is performed. The influence of the interface on the EET times (via the donor fluorescence lifetime, eq 5) depends strongly on the molecular orientation relative to the interface. Because of our selection, only molecules oriented preferentially parallel to the interface are investigated, corresponding to a rather restricted influence of the interface on the EET times. From this, we estimated the variations of the EET times to be on the order of $\pm 6\%$, significantly smaller than the experimentally observed distribution shown in Figure 4. That is, interfacial effects are rather unlikely for explaining the observed discrepancy.

It has been stressed by several authors that the point-dipole approximation used in standard Förster theory is expected to be inadequate at short distances, particularly when the effective spatial extension of the electronic excitations of donor and acceptor are on the order of the intermolecular distance.^{34–37} That is, the proximity of donor and acceptor relative to their spatial dimensions could be a dominating contribution to the observed discrepancy between simple Förster theory and our experimental data. Further deviations from ideal theory are expected if through bond mediated exchange via bridging groups is involved.¹ In this context, we do not refer to π conjugation to the bridge because quantum chemical calculations have clearly shown²⁶ that the phenyl rings adjacent to the chromophores are oriented orthogonal to the chromophore planes. Although both effects discussed in this section could play a role in our dyad, definitive conclusions cannot be drawn at present.

Conclusions

We have investigated a novel donor/acceptor dyad, in which the energy transfer efficiency was adjusted to observe donor as well as acceptor emission. A significantly smaller photostability of the donor allowed for time-resolved measurements of the acceptor emission with and without energy transfer from the donor. This behavior allows us to determine energy transfer times with high accuracy, even though they are significantly shorter than the temporal resolution of our setup. Our experimental observations indicate deviations from model calculations based on standard Förster theory. Further experimental and theoretical investigations are needed to substantiate this preliminary result and the origin of these deviations. Particularly, the knowledge and comparison of emission lifetimes, intensity ratios (PDI-TDI), and the spectral positions of the individual single-molecule spectra will allow for further quantifying of the energy transfer process. Because of the rigid structure of our model system, it will be a good candidate for a meaningful comparison to extended EET theory.

Acknowledgment. We would like to thank C. Hübner for helpful suggestions at the early stages of this work. Financial

support by the Deutsche Forschungsgemeinschaft (SFB 625) is gratefully acknowledged.

References and Notes

- (1) Scholes, G. D. *Annu. Rev. Phys. Chem.* **2003**, *54*, 57.
- (2) Webber, S. E. *Chem. Rev.* **1990**, *90*, 1469.
- (3) Friend, R. H.; Gymer, R. W.; Holmes, A. B.; Burroughes, J. H.; Marks, R. N.; Taliani, C.; Bradley, D. D. C.; Dos Santos, D. A.; Bredas, J. L.; Logdlund, M.; Salaneck, W. R. *Nature* **1999**, *397*, 121.
- (4) Sundstrom, V.; Pullerits, T.; van Grondelle, R. *J. Phys. Chem. B* **1999**, *103*, 2327.
- (5) Balzani, V.; Ceroni, P.; Maestri, M.; Vicinelli, V. *Curr. Opin. Chem. Biol.* **2003**, *7*, 657.
- (6) Foerster, T. *Discuss. Faraday Soc.* **1959**, *27*, 7.
- (7) Stryer, L.; Haugland, R. P. *Biochemistry* **1967**, *58*, 719.
- (8) Drake, J. M.; Klafter, J.; Levitz, P. *Science* **1991**, *251*, 1574.
- (9) Dahan, M.; Deniz, A. A.; Ha, T. J.; Chemla, D. S.; Schultz, P. G.; Weiss, S. *Chem. Phys.* **1999**, *247*, 85.
- (10) Deniz, A. A.; Laurence, T. A.; Beligere, G. S.; Dahan, M.; Martin, A. B.; Chemla, D. S.; Dawson, P. E.; Schultz, P. G.; Weiss, S. *Proc. Natl. Acad. Sci. U.S.A.* **2000**, *97*, 5179.
- (11) Margittai, M.; Widengren, J.; Schweinberger, E.; Schroder, G. F.; Felekyan, S.; Hausteiner, E.; Konig, M.; Fasshauer, D.; Grubmuller, H.; Jahn, R.; Seidel, C. A. M. *Proc. Natl. Acad. Sci. U.S.A.* **2003**, *100*, 15516.
- (12) Hettich, C.; Schmitt, C.; Zitzmann, J.; Kuhn, S.; Gerhardt, I.; Sandoghdar, V. *Science* **2002**, *298*, 385.
- (13) Christ, T.; Petzke, F.; Bordat, P.; Herrmann, A.; Reuther, E.; Mullen, K.; Basche, T. *J. Lumin.* **2002**, *98*, 23.
- (14) Hofmann, C.; Ketelaars, M.; Matsushita, M.; Michel, H.; Aartsma, T. J.; Kohler, J. *Phys. Rev. Lett.* **2003**, *90*, art. no. 013004.
- (15) Hofkens, J.; Cotellet, M.; Vosch, T.; Tinnefeld, P.; Weston, K. D.; Ego, C.; Grimsdale, A.; Mullen, K.; Beljonne, D.; Bredas, J. L.; Jordens, S.; Schweitzer, G.; Sauer, M.; De Schryver, F. *Proc. Natl. Acad. Sci. U.S.A.* **2003**, *100*, 13146.
- (16) Hubner, C. G.; Zumofen, G.; Renn, A.; Herrmann, A.; Mullen, K.; Basche, T. *Phys. Rev. Lett.* **2003**, *91*, art. no. 093903.
- (17) Lippitz, M.; Hubner, C. G.; Christ, T.; Eichner, H.; Bordat, P.; Herrmann, A.; Mullen, K.; Basche, T. *Phys. Rev. Lett.* **2004**, *92*, art. no. 103001.
- (18) Ha, T.; Enderle, T.; Ogletree, D. F.; Chemla, D. S.; Selvin, P. R.; Weiss, S. *Proc. Natl. Acad. Sci. U.S.A.* **1996**, *93*, 6264.
- (19) Mais, S.; Tittel, J.; Basche, T.; Brauchle, C.; Gohde, W.; Fuchs, H.; Muller, G.; Mullen, K. *J. Phys. Chem. A* **1997**, *101*, 8435.
- (20) Kircher, T.; Lohmannsroben, H. G. *Phys. Chem. Chem. Phys.* **1999**, *1*, 3987.
- (21) Schweitzer, G.; Gronheid, R.; Jordens, S.; Lor, M.; De Belder, G.; Weil, T.; Reuther, E.; Mullen, M.; De Schryver, F. C. *J. Phys. Chem. A* **2003**, *107*, 3199.
- (22) Hubner, C. G.; Ksenofontov, V.; Nolde, F.; Mullen, K.; Basche, T. *J. Chem. Phys.* **2004**, *120*, 10867.
- (23) Cotellet, M.; Gronheid, R.; Habuchi, S.; Stefan, A.; Barbafina, A.; Mullen, K.; Hofkens, J.; De Schryver, F. C. *J. Am. Chem. Soc.* **2003**, *125*, 13609.
- (24) Metivier, R.; Kulzer, F.; Weil, T.; Müllen, K.; Basche, T. *J. Am. Chem. Soc.* **2004**, *126*, 14363.
- (25) Nolde, F.; Müllen, K., in preparation, 2005.
- (26) Diezemann, G.; Gauss, J. Unpublished results; calculations were performed by density functional theory (DFT) using Becke-Perdew (BP) functional (Becke, A. D. *Phys. Rev. A* **1988**, *38*, 3098; Perdew, J. P. *Phys. Rev. B* **1986**, *33*, 8822) and a polarized split-valence (SVP) basis (Schäfer, A.; Horn, H.; Ahlrichs, R. *J. Chem. Phys.* **1992**, *97*, 2571–2577).
- (27) Lakowicz, J. R. *Principle of Fluorescence Spectroscopy*; Kluwer Academic/Plenum Publishing Corporation: New York, 1999.
- (28) Macklin, J. J.; Trautman, J. K.; Harris, T. D.; Brus, L. E. *Science* **1996**, *272*, 255.
- (29) Haase, M.; Hübner, C. G.; Eichner, H.; Nolde, F.; Müllen, K.; Basché, T., in preparation, 2005.
- (30) Würthner, F. *Chem. Commun.* **2004**, 1564.
- (31) Lukosz, W.; Kunz, R. E. *J. Opt. Soc. Am.* **1977**, *67*, 1607.
- (32) Lee, M.; Tang, J. Y.; Hochstrasser, R. M. *Chem. Phys. Lett.* **2001**, *344*, 501.
- (33) Vallee, R.; Tomczak, N.; Gersen, H.; van Dijk, E. M. H. P.; Garcia-Parajo, M. F.; Vancso, G. J.; van Hulst, N. F. *Chem. Phys. Lett.* **2001**, *348*, 161.
- (34) Wong, K. F.; Bagchi, B.; Rossky, P. J. *J. Phys. Chem. A* **2004**, *108*, 5752.
- (35) Krueger, B. P.; Scholes, G. D.; Fleming, G. R. *J. Phys. Chem. B* **1998**, *102*, 5378.
- (36) Beljonne, D.; Cornil, J.; Silbey, R.; Millie, P.; Bredas, J. L. *J. Chem. Phys.* **2000**, *112*, 4749.
- (37) Murrell, J. N.; Tanaka, J. *Mol. Phys.* **1964**, *7*, 363.